

Accepted Manuscript

Full Length Article

Incorporation of the zosteric sodium salt in silica nanocapsules: synthesis and characterization of new fillers for antifouling coatings

Ludovica Ruggiero, Laura Crociani, Elisabetta Zendri, Naida El Habra, Paolo Guerriero

PII: S0169-4332(17)33876-X
DOI: <https://doi.org/10.1016/j.apsusc.2017.12.228>
Reference: APSUSC 38098

To appear in: *Applied Surface Science*

Received Date: 26 April 2017
Revised Date: 4 December 2017
Accepted Date: 27 December 2017

Please cite this article as: L. Ruggiero, L. Crociani, E. Zendri, N. El Habra, P. Guerriero, Incorporation of the zosteric sodium salt in silica nanocapsules: synthesis and characterization of new fillers for antifouling coatings, *Applied Surface Science* (2017), doi: <https://doi.org/10.1016/j.apsusc.2017.12.228>

This is a PDF file of an unedited manuscript that has been accepted for publication. As a service to our customers we are providing this early version of the manuscript. The manuscript will undergo copyediting, typesetting, and review of the resulting proof before it is published in its final form. Please note that during the production process errors may be discovered which could affect the content, and all legal disclaimers that apply to the journal pertain.



1 Incorporation of the zosteric sodium salt in silica nanocapsules: 2 synthesis and characterization of new fillers for antifouling 3 coatings

4 Ludovica Ruggiero^{1,2,4}, Laura Crociani^{3,4}, Elisabetta Zendri¹, Naida El Habra³, Paolo Guerriero³

5 ¹ Dipartimento di Scienze Ambientali, Informatica e Statistica (DAIS), Università Ca' Foscari – Venezia, Via Torino 155/b, 30175
6 Mestre – VE

7 ² Dipartimento di Scienze, Università degli Studi Roma Tre, Via della Vasca Navale 84, 00146 Roma - RM, Italy

8 ³ Istituto di Chimica della Materia Condensata e delle Tecnologie per l'Energia, ICMATE, CNR, C.so Stati Uniti 4, 35127 Padova

9 Email address: ludovica.ruggiero@gmail.com, laura.crociani@cnr.it

10 Abstract

11 In the last decade many commercial biocides were gradually banned for toxicity. This work reports, for the
12 first time, the synthesis and characterization of silica nanocontainers loaded with a natural product
13 antifoulant (NPA), the zosteric sodium salt which is a non-commercial and environmentally friendly product
14 with natural origin. The synthesis approach is a single step dynamic self-assembly with tetraethoxysilane
15 (TEOS) as silica precursor. Unlike conventional mesoporous silica nanoparticles, the structure of these silica
16 nanocontainers provides loading capacity and allows prolonged release of biocide species. The obtained
17 nanocapsules have been characterized morphologically by scanning electron microscopy (SEM) and
18 transmission electron microscopy (TEM). The encapsulation was checked by FTIR ATR spectroscopy and
19 thermogravimetric analyses. **The results of the release studies show the great potential of the here
20 presented newly developed nanofillers in all applications where a controlled release of non-toxic and
21 environmentally friendly biocides is required.**

22 **KEYWORDS:** Zosteric sodium salt, environmentally friendly biocide, encapsulation of biocides, silica
23 nanoparticles, TEOS

24 HIGHLIGHTS

- 26 • Design of a new system to reduce the amount of biocide in antifouling coatings
- 27 • A single step self-assembly method to encapsulate environmentally friendly biocide
- 28 • Successful encapsulation of the zosteric sodium salt in silica nanocapsules

⁴ Authors to whom any correspondence should be addressed

29

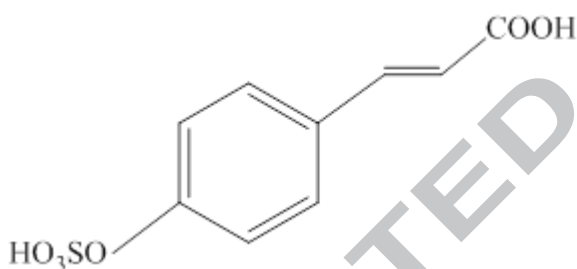
30 **1.Introduction**

31 Biofouling has frequently been reported for any kind of material from stone surfaces such as building
32 facades, historical monuments and outdoor artworks to metallic surface, such as ship-hull or industrial
33 platform. **Those surfaces are inevitably exposed to the weather that contributes to create a suitable
34 combination of factors necessary for the algal growth (e.g. dampness, warmth and light) [1].**

35 Biofouling involves many living organisms (bacteria, fungi, algae, cyanobacteria, mosses, ferns and higher
36 plants), **with the formation of complex systems (biofilms) [2]. To overcome biofouling, two different
37 strategies can be used: i) acting on the bioreceptivity of the substrates; ii) applying antifouling agents
38 on the substrates. The first approach provides the application of products that weaken the link
39 between the cells of the microorganisms and the exposed surface. The most promising material is
40 titanium dioxide (TiO₂). Under ultraviolet (UV) exposure, TiO₂ becomes superhydrophilic and creates
41 a film on treated surfaces that changes the bioreceptivity of the substrates. One of the most
42 controversial aspect of TiO₂ coatings when applied on stones is their durability. Recent investigation
43 on the latter - in the specific case of TiO₂ nanotreatments on architectural stones - shows in fact a very
44 limited time efficiency of the superhydrophilic and hydrophilic treatment that thus becomes quite
45 short-life because of the quick degradation of the coatings [3].**

46 **According to the second approach,** antifouling agents can be traditionally applied in various forms (spray,
47 compresses soaking, brushing, etc.) or added to coating formulations applied to protect substrates against
48 biological colonization. Generally, when the biocides are added into the coating formulations, the antifouling
49 action usually becomes quite short-lived, because of the premature release or the degradation of the active
50 substance. Most biocides are small molecules and hence subject to fast self-diffusion in the coating matrix.
51 As a consequence, this simple approach requires the use of very high concentrations of the biocide in order
52 to maintain the antifouling function for a long time [4]. The use of excessive amounts of biocide may pollute
53 the environment and, if the biocide is incompatible with the used matrix, it may also induce a macroscopic
54 phase separation in the coating film [5]. The encapsulation/entrapment of biocides in nanocapsules to control
55 the release of bioactive species is a good approach to reduce the amount of biocide and to obtain a
56 satisfactory long-action antifouling coating increase.

57 Many early antifouling substances consisting of organo-mercury, lead and dichloro-diphenyltrichloroethane
58 (DDT) posed severe environmental and human health risks [6-9]. Considerable studies were made to
59 implement and evaluate alternative antifoulants with better environmental compatibility [10]. The European
60 directive 98/8/CE highlights the important contributions offered by the natural product antifoulants (NPAs)
61 as non- or less toxic alternatives to traditional biocides [11]. Among the NPAs the zosteric acid (ZA), or p-
62 (sulfoxy) cinnamic acid (figure 1), is proposed as an alternative biocide suitable for preventive or integrative
63 anti-biofilm approaches. The zosteric acid was first extracted from the *Zostera marina*. Marine plants are
64 constantly exposed to harmful attacks by bacteria, spores or fungi building biofilms on the plant surfaces
65 [12-13]. In order to protect itself the seagrass *Zostera marina* produces and continuously releases the water-
66 soluble zosteric acid. The antifouling capability of the zosteric acid and its sodium salt was attributed to the
67 sulfate group present in these compounds [14]. These antifoulants bind the attachment sites on cell surfaces
68 at non-toxic concentrations inhibiting the adhesion of the microorganism interfering with key-steps
69 orchestrating biofilm formation [15-16].



70
71 **Figure 1.** Structure formula of the zosteric acid (p-(sulfo-oxy) cinnamic acid).

72 At present, the possibility to realize the entrapment of NPAs in coatings formulations or their encapsulation
73 to control the release have not been sufficiently addressed. **In this work we focused on the encapsulation**
74 **of zosteric sodium salt to create an innovative filler with controlled-release properties for antifouling**
75 **coatings. We decided to test the not commercial zosteric sodium salt, derivative of the zosteric acid, in**
76 **accordance to the pro-ecological trends and EU regulations. We compared the results of zosteric**
77 **sodium salt encapsulation with the encapsulation of sodium benzoate (BS), a commercial biocide used**
78 **in many areas from cultural heritage to food preservatives.** These compounds were encapsulated in silica
79 nanocapsules through a single step dynamic self-assembly synthesis approach [17].

80 2. Experimental procedure

81 2.1. Materials

82 The active compounds used for encapsulation were sodium benzoate (BS) (Aldrich) and the zosteric sodium
83 salt (ZS). ZS was synthesized from *trans*-4-hydroxycinnamic and the sulphur trioxide pyridine complex.
84 Methyl zosteric ester (EZS) was synthesized according to the literature [16]. For the preparation of the
85 capsules, cetyltrimethylammonium bromide (CTAB, Aldrich), ammonia solution (NH₃_{aq}, Anala®),
86 tetraethoxysilane (TEOS, Aldrich) and diethyl ether (Et₂O, Aldrich) were used. All the chemicals were
87 analytic grade and were used without further purification.

88

89 *2.2. Encapsulation of the zosteric sodium salt in silica nanoparticles*

90 The synthesis of the silica nanocapsules was adapted from the procedure by Chen et al. [17] (Chen et al.
91 2008). Denionized water (35 ml) and CTAB (0.25 g) were stirred at 55 °C for 15 minutes. Following the
92 complete dissolution of CTAB, 0.25 ml of ammonia solution (25-28 %) were added into the mixture under
93 continued stirring and heating. Afterward, a ZS solution in methanol (5 ml, 1.3 % in wt) dissolved in 25 ml
94 of diethyl ether was added to the aqueous solution under constant stirring. After 30 minutes, when the oil-in-
95 water (O/W) emulsion was stabilized, 1.25 ml of TEOS was dripped slowly to the emulsion. The reaction
96 was left at room temperature for 24h under constant stirring. The resulting precipitates were filtered under
97 vacuum, repeatedly washed (in deionized water) and dried at room temperature. The encapsulation of BS
98 was performed in the same way. A small portion of these materials were calcined at 550 °C for 5h in order to
99 remove CTAB and other organic components, on which the amount of the loaded biocide was determined.

100

101 *2.3. Silica nanoparticles characterization*

102 The **morphology** and dimensions of the nanoparticles were studied via scanning and transmission electron
103 microscopy using a EG-ESEM FEI Quanta 200 F instrument equipped with a field emission gun, operating
104 both in high and low (120 Pa) vacuum conditions and using a JEOL JEM 3010 operating at 300 KV,
105 respectively. All the samples were sputtered with graphite before observations. **Particle size distribution**
106 **was determined using the “ImageJ” software for image processing** [18]. FTIR experiments were carried
107 out on a Nicolet Nexus 750 equipped with the ATR system. Thermogravimetric analysis (TG/DTA) was
108 carried out under air atmosphere, with a heating rate of 5°C min⁻¹ from room temperature up to 800 °C, using
109 the NETZSCH STA 449 TG/DTA analyzer.

110

111 2.4. Release studies of the biocides

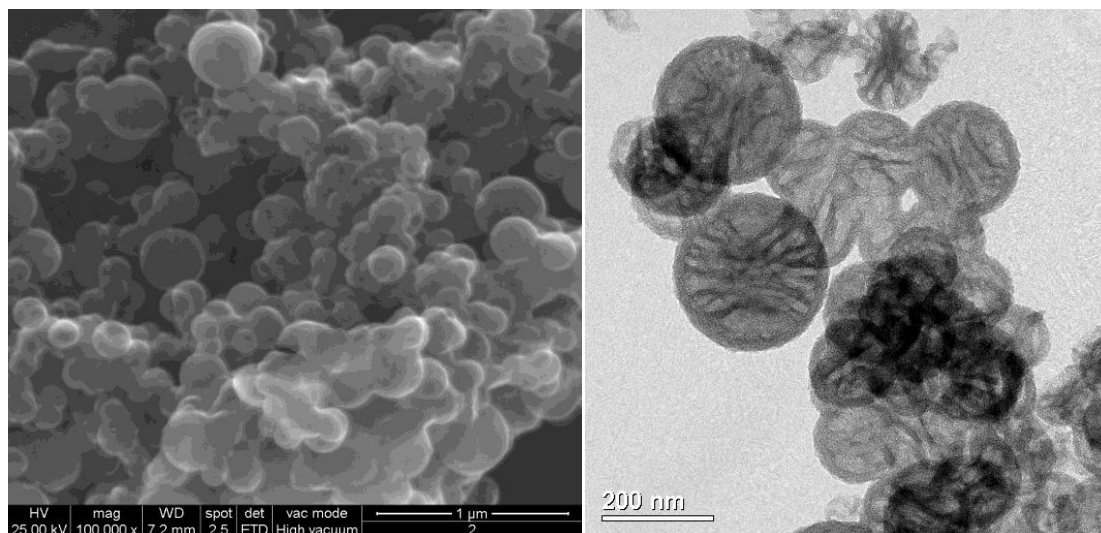
112 The release of the biocides was monitored by UV-Vis spectrophotometry (Unicam UV500) in the range of
113 200-650 nm by dispersing 15 mg of silica nanocapsules loaded with zosteric sodium salt and with sodium
114 benzoate in 5 ml of ethanol separately. The suspensions were slowly stirred (93 rpm) at room temperature. A
115 3 ml sample of the mixture was collected with a syringe and analysed by UV-Vis spectrophotometry at given
116 time intervals, being no filtering process performed because of the clarity of the suspensions. After
117 measurement the extracted mixture was added back to the initial ethanol mixture. The correlation coefficient
118 of the calibration curves obtained with 5 standards was higher than 0.99. The aliquots collected to quantify
119 light emission were also used to quantify the amount of the biocide released in solution.

120

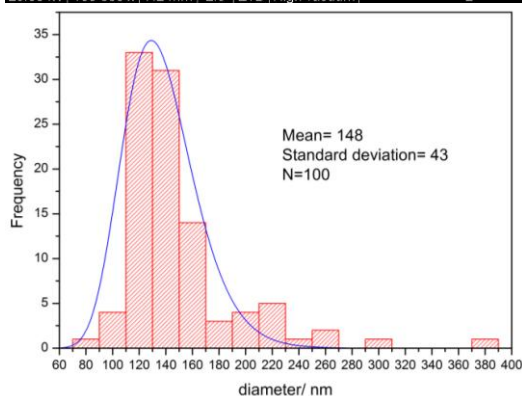
121 3. Results and discussion

122 In this research it was used a single step method to obtain the silica nanocontainers. This encapsulation
123 procedure used TEOS condensation at the oil-in-water miniemulsion interface. Diethyl ether has the
124 important role of porogen, cosolvent and template with CTAB for silica shell formation [19]. To successfully
125 encapsulate the hydrophilic zosteric sodium salt some adjustments were performed and here reported for the
126 first time. First, an organic solvent in which ZS was soluble and miscible with the organic phase of the
127 miniemulsion was selected. According to the literature, the solubility of zosteric acid in methanol was found
128 to be 1.3% [20] and methanol was used to solubilise the sodium salt in order to hinder its complete
129 dissolution in the water phase of the O/W miniemulsion during the nanocapsule formation and hardening.
130 Sodium benzoate was analogously encapsulated using the same amount of biocide.

131 In order to analyse the morphology of the synthesized nanoparticles, SEM and TEM analyses were
132 performed. Typical SEM and TEM **images** of the empty silica nanocapsules (NC) are shown in figure 2 a
133 and b. Clearly, they consist of spherical particles with a regular shape. TEM micrographs show that shells of
134 these nanocapsules have a thickness of ca 11 nm and have a porous structure with clearly distinguished
135 pleats. According to previous studies, the spherical nanoparticles have a hollow nature, as revealed by the
136 contrast between the dark edge and the pale centre [17].



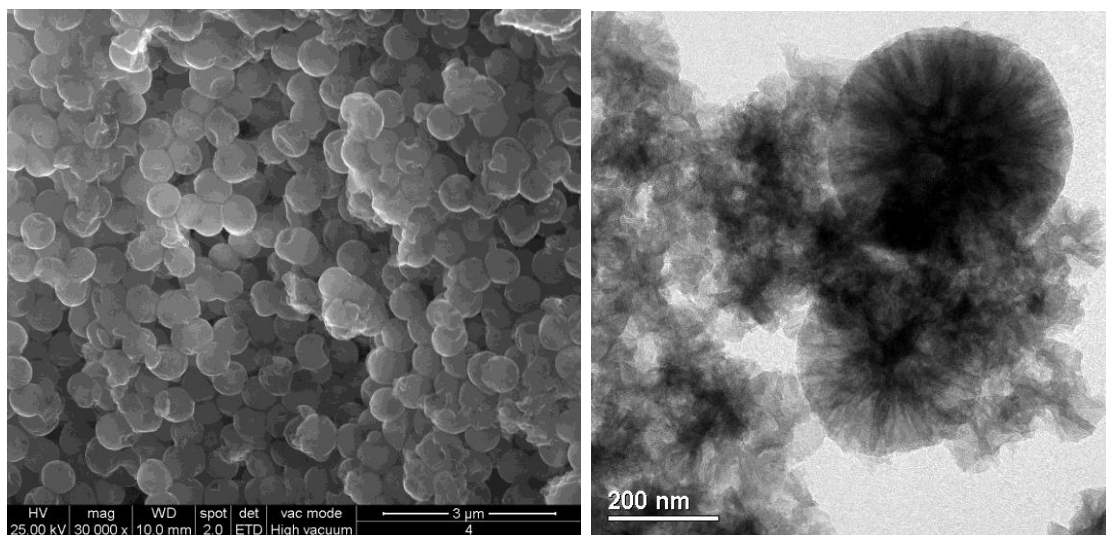
137



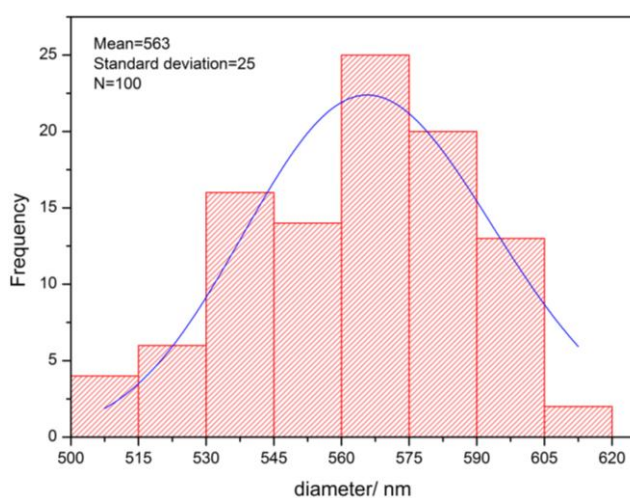
138

139 **Figure 2.** (a) SEM and (b) TEM micrographs of the empty silica nanocapsules (NC) and (c) **histograms**
 140 **with size distribution determined with ImageJ.**

141 Comparing the empty nanocapsules (NC) with the nanocapsules loaded with the different biocides, it is
 142 possible to verify that the encapsulation did not promote any changes in shape, but in size only. **NC have a**
 143 **size distribution centered at 148 nm with a standard deviation of 43 nm for 100 measurements, as**
 144 **reported in Figure 2c. Containers loaded with ZS seem to be larger than the empty ones (Figure 3 a**
 145 **and b), resulting in a size distribution centered at 563 with a standard deviation of 25 for 100**
 146 **measurements (Figure 3 c).**



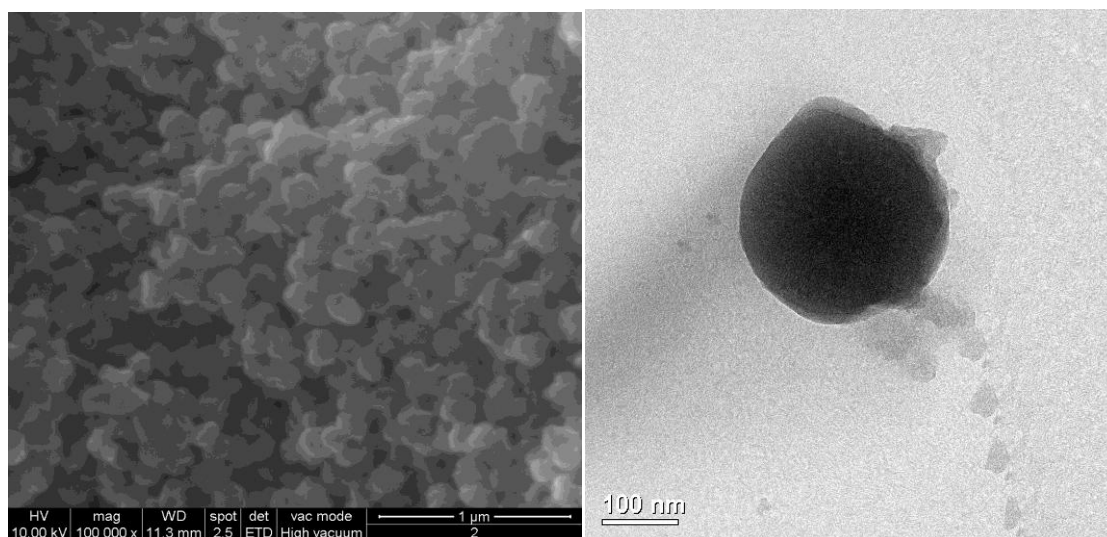
147



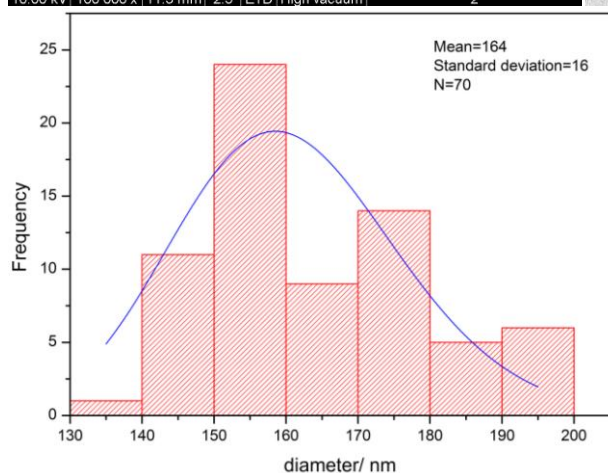
148

149 **Figure 3.** (a) SEM and (b) TEM micrographs of the silica nanocapsules loaded with the zosteric sodium salt
 150 (NC-ZS) and (c) histograms with size distribution determined with ImageJ.

151 **Instead, when the encapsulation of BS was performed, no significant variation in the size distribution**
 152 **of empty capsules was observed (Figure 4 a and b). The NC-BS have a size distribution centered at**
 153 **164 nm with a standard deviation of 16 nm for 70 measurements (Figure 4 c). Due to the organic**
 154 **residual, the nanoparticles of both samples appear agglomerated (figure 2-4).**



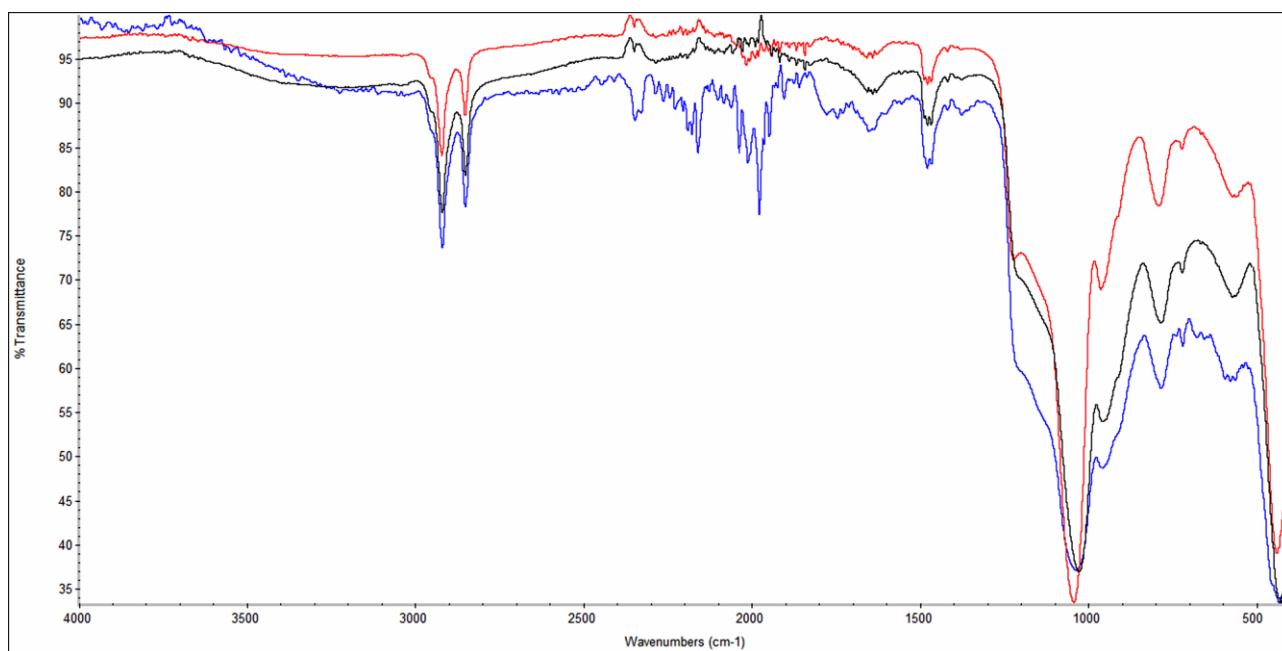
155



156

157 **Figure 4. (a) SEM and (b) TEM micrographs of the nanocontainers with BS (NC-BS) and (c) histograms**
 158 **with size distribution determined with ImageJ.**

159 FTIR analyses were performed in order to confirm the presence of the biocides in the nanocontainers. The
 160 FTIR spectrum of the empty silica nanoparticles (figure 5) shows the typical absorbance bands associated
 161 with amorphous silica, in particular the 470 cm^{-1} bending peak, the 800 cm^{-1} and 1040 cm^{-1} stretching peaks
 162 of the Si-O-Si group [21]. In this spectrum several characteristic bands associated with CTAB can be
 163 observed: $\nu_{\text{as}}(\text{CH}_3)$ and $\nu_{\text{sym}}(\text{CH}_3)$ at 2943 and 2870 cm^{-1} , $\delta(\text{CH}_2)$ mode at 1462 and 1472 cm^{-1} and the δ_{sym}
 164 ($\text{N}-\text{CH}_3$) and $\nu(\text{C}-\text{N})$ at 1396 and 912 cm^{-1} , respectively [22]. In the case of the nanoparticles loaded with
 165 the zosteric sodium salt (NC-ZS) (figure 5), the presence of ZS is confirmed by the bands observed at 1645
 166 cm^{-1} , which are associated with the stretching mode of C=O [23]. The enlarged band centered at 1028 cm^{-1}
 167 due to the $\nu(\text{Si}-\text{O}-\text{Si})$ has a shoulder at 1220 cm^{-1} , which is associated with $\nu_{\text{as}}(\text{S}=\text{O})$ signal, relative to the
 168 sulfate group present in the zosteric sodium salt. In the case of the nanoparticles loaded with sodium
 169 benzoate (NC-BS) (figure 5), the encapsulation of BS is confirmed by the bands at 1601 cm^{-1} and 1406 cm^{-1} ,
 170 which are associated with the ν_{as} and $\nu_{\text{sym}}(\text{COO}^-)$, respectively [24].

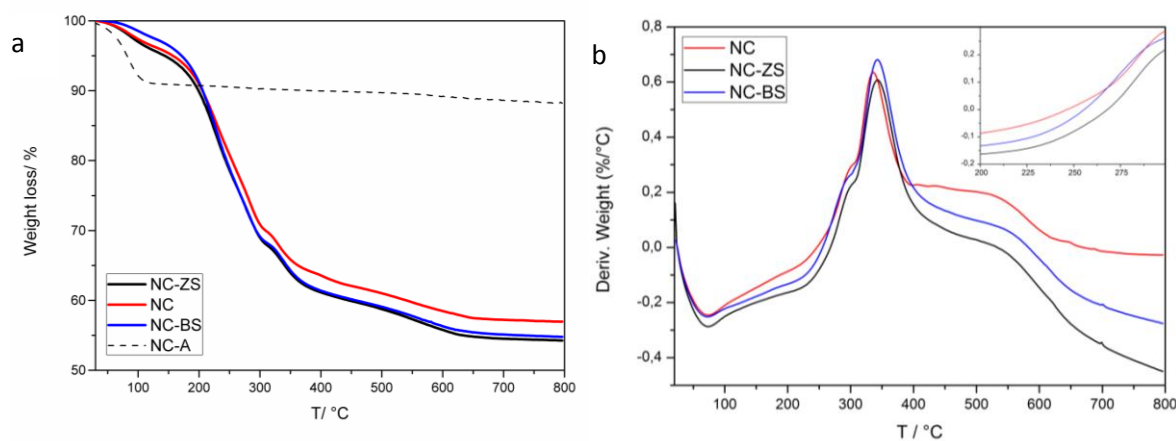


171

172 **Figure 5.** FTIR spectrum of NC-BE (blue line), NC-ZS (black line), NC (red line).

173 To verify the thermal stability of the silica nanocontainers and to quantify the amount of the encapsulated
174 biocides, thermogravimetric tests were carried out. In agreement with the literature the calcined empty silica
175 nanocontainers do not show significant variation with temperature.

176 Comparing the not calcined silica nanoparticles (NC) with the calcined ones (NC-A), the total weight loss is
177 31%. This value is relative to the degradation of non-hydrolysed/condensed TEOS and to the removal of the
178 organic fraction comprising the cationic surfactant CTAB [25]. The curves corresponding to the capsules
179 with ZS and BS show a similar profile to that of the empty capsules, except in the range between 200 and
180 300 °C, as evidenced by the derivatives of thermogravimetric curves (Figure 6 b). In this range a weight
181 lost is more pronounced and is attributed to desorption of the biocides degrading in this range of temperature
182 (figure 6) [26-27].



183

184 Figure 6. (a) Thermogravimetric curves and (b) their derivatives of the calcined empty nanocapsules (NC-A),
 185 the not calcined ones – (NC) and those encapsulating ZS (NC-ZS) and BS (NC-BS). **The insert in figure 6**
 186 **b shows the enlarged area between 200 and 300 °C.**

187 It is interesting to use the difference of mass loss between the loaded and empty capsules to estimate the
 188 amount of biocide loading, 3.2% in the case of NC-ZS and 2.6% for NC-BS.

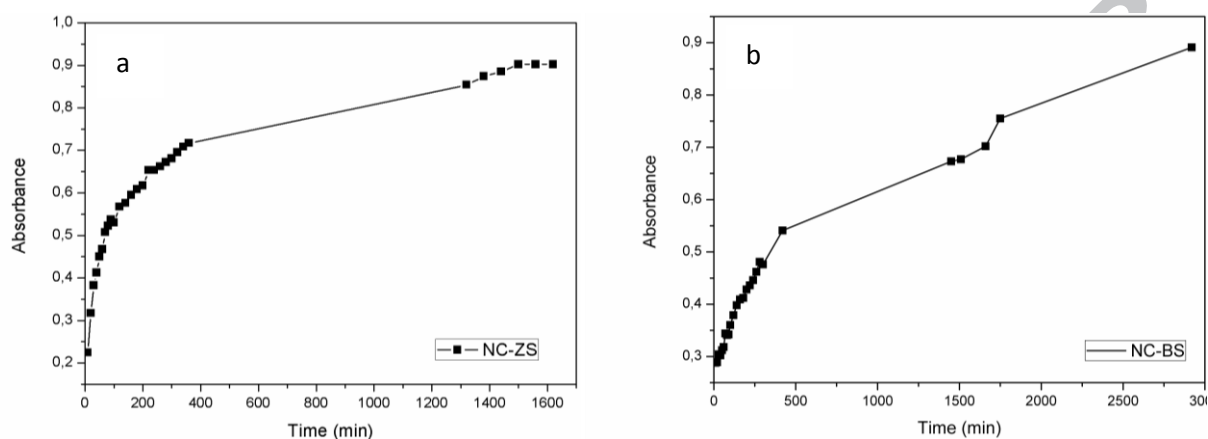
189 Analogously to a previous work [19], the controlled release of ZS and BS from the silica nanocontainers
 190 dispersed in ethanol was examined by means of UV-Vis spectrophotometry at different times. The release
 191 process was monitored by following the absorption change of the ethanol media in the range of 200-650 nm
 192 after removal of the silica nanoparticles. A kinetic release curve (**shown in** figure 7) was plotted by using the
 193 absorption of the peak at ca. 267 nm for ZS and at 223 nm for BS. **The releasing process of ZS initially**
 194 **proceeded fast (figure 7a), then gradually slowed and levelled off after 22 h; actually nearly 52% of ZS**
 195 **as estimated via the following equation [17]:**

$$196 \text{ (1) Cumulative release (\%)} = \frac{Ab_{st}}{Abs_{max}} \times 100$$

197 (where Abs_{max} is the absorbance of the peak at ca. 267 nm at 26h after which the peak intensity no
 198 longer changed; Ab_{st} is the absorbance of the same peak recorded at time t) was released into ethanol
 199 in 1h. In the case of BS, the process does not level off after 50 h and after 1h the 34% of BS (estimated
 200 from eq 1. at ca 223 nm at 50 h) was released into ethanol. According to the literature data, these release
 201 results indicated that the encapsulation and controlled release of the organic molecule has been realized.
 202 Once the nanocapsules are dispersed in ethanol, a fraction of the biocide is released until equilibrium
 203 between biocide in the nanocapsule and in the ethanol phase is reached. The differences in the release

204 profiles of biocides are probably due to their different solubility in ethanol. Furthermore, it is possible that
 205 during the synthesis ZS and BS are encapsulated in different region of the nanoparticles (core vs shell). As
 206 particles were repeatedly washed prior to the characterisation procedure, either ZS or BS are definitely in the
 207 core of the particles or in the porous silica shell.

208



209

210 **Figure 7.** Release profiles of the nanocapsules loaded with ZS (a) and BS (b).

211 To verify that the release proceeded by diffusion of guest molecules into ethanol through the shells of
 212 nanocapsules, we decided to study the release of another sample, in which methyl zosteric ester (EZS) [28]
 213 was physically adsorbed on silica. However, when this sample was dispersed in ethanol to perform the
 214 release studies, the cumulative release of EZS was 97%, after 1h. This result shows that BS and ZS
 215 encapsulated by one-step miniemulsion process were mostly allocated in the core or in the shell structure of
 216 nanoparticles providing a good prolonged release.

217 4. Conclusion

218 The present paper reported, for the first time, the encapsulation of the zosteric sodium salt in silica
 219 nanocapsules combining two innovative research lines: the use of environmentally friendly antibiofouling
 220 agent and the one-step encapsulation method. The known biocide effect of the zosteric sodium salt makes the
 221 developed nanomaterial a promising engineering system with application in antifouling coating on an
 222 outdoor surface. The synthesized nanomaterials were thermally stable with a regular and spherical shape.
 223 The size of the obtained materials were influenced by the molecular size of the biocides. The loading content
 224 of ZS and BS were found to be 3.2 and 2.6 wt%, respectively.

225 The preliminary release studies in ethanol showed that the release of ZS was relatively gradual but after 22
226 hours it was levelled off, while the releasing process of BS was still on after 50 hours.

227 The nanocontainers synthesized in this work were designed to be one component of a more complex
228 antifouling coating system, namely supercoating so that it will be interesting to evaluate the effectiveness of
229 free zosteric sodium salt free as well as encapsulated in silica nanocontainers in water-based and solvent-
230 based coatings.

231

232 **Acknowledgments**

233 The authors would like to thank dr. A. Galenda for his suggestions on UV spectra, dr. D. Cristofori for TEM
234 images and dr. Davide Barsotti for the synthesis of the sodium zosteric salt.

235 **References**

- 236 [1] **J.M.P.Q. Delgado, *New Approaches to Building Pathology and Durability*, Springer 2016,**
237 **Photocatalytic TiO₂ Nano-Coating for Biofouling prevention of Clay Facedes 159-177**
- 238 [2] F. Borderie, B. Alaoui-Sossé and L. Aleya, Heritage materials and biofouling mitigation through UV-
239 C irradiation in show caves: state-of-the-art practices and future challenges, *Environ Sci Pollut Res*
240 22 (2015) 4144-72
- 241 [3] **J. Drelich, E. Chibowski, D. Desheng Meng and K. Terpilowski, *Hydrophilic and***
242 **superhydrophilic surfaces and materials, *Soft Matter* 7 (2011) 9804-9828**
- 243 [4] M. A. Trojer, L. Nordstierna, J. Bergek, H. Blanck, K. Holmberg and M. Nydéna, Use of
244 microcapsules as controlled release devices for coatings, *Advances in Colloid and Interface Science*
245 222 (2015) 18–43
- 246 [5] S. K. Ghosh, *Functional Coatings and Microencapsulation: A General Perspective in Functional*
247 *Coatings by Polymer Microencapsulation*, 2006 *WILEY-VCH Verlag GmbH & Co. KGaA Weinheim*
248 1-25
- 249 [6] M. Simões, L. C. Simões and M. J. Vieira, A review of current and emergent biofilm control
250 strategies, *LWT Food Sci. Technol.* 43 (2010) 573–583

- 251 [7] J. E. Gittens, T. J. Smitha, R. Suleiman and R. Akid, Current and emerging environmentally-friendly
252 systems for fouling control in the marine environment, *Biotechnol. Adv.* 31 (2013) 1738–1753
- 253 [8] D. Pinna, B. Salvadori, M. Galeotti, Monitoring the performance of innovative and traditional
254 biocides mixed with consolidants and water-repellents for the prevention of biological growth on
255 stone, *Science of the Total Environment* 423 (2012) 132–141
- 256 [9] R. Carrillo-González, M. Araceli Martínez-Gómez, M. C. A. González-Chávez, J. C. Mendoza
257 Hernández, Inhibition of microorganisms involved in deterioration of an archaeological site by silver
258 nanoparticles produced by a green synthesis method, *Science of the Total Environment* 565 (2016)
259 872–881
- 260 [10] J. Walentowska and J. Foksowicz-Flaczyk, Thyme essential oil for antimicrobial protection of natural
261 textiles, *International Biodeterioration & Biodegradation* 84 (2013) 407-411
- 262 [11] European parliament 1998 Directive of the European Parliament and of the council of 16 February
263 1998 concerning the placing of biocidal products on the market European Union: Official Journal of
264 the European Communities 24 th April 1998 61
- 265 [12] T. Geiger, P. Delavy, R. Hany, J. Schleuniger and M. Zinn, Encapsulated Zosteric Acid Embedded in
266 Poly[3-hydroxyalkanoate] Coatings - Protection against, *Biofouling Polymer Bulletin* 52 (2004) 65-
267 72
- 268 [13] M. Boopalan and A. Sasikumar, Studies on Biocide Free and Biocide Loaded Zeolite Hybrid Polymer
269 Coatings on Zinc Phosphated Mild Steel for the Protection of Ships Hulls from Biofouling and
270 Corrosion, *Silicon* 3 (2011) 207–214
- 271 [14] B. Zhang Newby, Cutright T, C. A. Barrios and Q. Xu, Zosteric Acid—An Effective Antifoulant for
272 reducing fresh water bacterial attachment on coatings, *JCT Research* 3 (2006) 69-70
- 273 [15] M. H. Fletcher, M. C. Jennings and W. M. Wuest, Draining the moat: disrupting bacterial biofilms
274 with natural products, *Tetrahedron* 70 (2014) 6373-6383
- 275 [16] F. Villa, B. Pitts, P. S. Stewart, B. Giussani, S. Roncoroni, D. Albanese, C. Giordano and M. Tunesi,
276 Efficacy of zosteric acid sodium salt on the yeast biofilm model *Candida albicans*, *Microb Ecol* 62
277 (2011) 584-598
- 278 [17] H. Chen, J. He, H. Tang and C. Yan, Porous Silica Nanocapsules and Nanospheres: Dynamic Self-
279 Assembly Synthesis and Application in Controlled Release, *Chem. Mater.* 20 (2008)5894–5900

- 280 [18] **W. Burger, M.J. Burge, Digital Image Processing: an Algorithmic Introduction Using Java,**
281 **Springer (2010)**
- 282 [19] F. Maia, A. P. Silva, S. Fernandes, A. Cunha, A. Almeida, J. Tedim, M. L. Zheludkevich and M. G.
283 S. Ferreira, Incorporation of biocides in nanocapsules for protective coatings used in maritime
284 applications, *Chemical Engineering Journal* 270 (2015) 150–157
- 285 [20] C. A. Barrios, Q. Xu, T. Cutright and B. Z. Newby, Incorporating zosteric acid into silicone coatings
286 to achieve its slow release while reducing fresh water bacterial attachment, *Colloids and Surfaces B:*
287 *Biointerfaces* 41 (2005) 83–93
- 288 [21] F. Maia, J. Tedim, A. D. Lisenkov, A. N. Salak, M. L. Zheludkevich and M. G. Ferreira, Silica
289 nanocontainers for active corrosion protection, *Nanoscale* 4 (2012) 1287–1298
- 290 [22] H. Badawy, J. Brunellière, M. Veryaskina, G. Brotons, S. Sablé, I. Lanneluc, K. Lambert, P.
291 Marmey, A. Milsted, T. Cutright, A. Nourry, J. Mouget and P. Pasetto, Assessing the Antimicrobial
292 Activity of Polyisoprene Based Surfaces, *Int. J. Mol. Sci.* 16 (2015) 4392-441
- 293 [23] R. B. Viana, A. B. F. da Silva and A. S. Pimentel, Infrared Spectroscopy of Anionic, Cationic, and
294 Zwitterionic Surfactants, *Advances in Physical Chemistry* 2012 1-15
- 295 [24] N. Kumar, S. Thomas, R. B. Tokas and R. J. Kshirsagar, Investigation on the adsorption
296 characteristics of sodium benzoate and taurine on gold nanoparticle film by ATR-FTIR spectroscopy
297 *Spectrochim Acta A Mol Biomol Spectrosc* 118 (2014) 614-8
- 298 [25] G. Sponchia, R. Marin, I. Freris, M. Marchiori, E. Moretti, L. Storaro, P. Caton, A. Lausi, A.
299 Benedetti and P. Riello, Mesoporous silica nanoparticles with tunable pore size for tailored gold
300 nanoparticles, *J Nanopart Res* 16 (2014) 2245- 2256
- 301 [26] G. Gorrasi, G. Attanasio, L. Izzo and A. Sorrentino, Controlled release mechanisms of sodium
302 benzoate from a biodegradable polymer and halloysite nanotube composite, *Polym Int* (66) 2017
303 690–698
- 304 [27] M. Boopalan and A. Sasikumar, Studies on biocide free and biocide loaded zeolite hybrid polymer
305 coatings on zinc phosphate mild steel for the protection of ships hulls from biofouling and corrosion,
306 *Silicon* 3 (2011) 207-214
- 307 [28] F. Villa, D. Albanese, B. Giussani, P. S. Stewart, D. Daffonchio and F. Cappitelli, Hindering biofilm
308 formation with zosteric acid, *Biofouling* 26 (2010) 739–752

